(2)

FINAL REPORT
OFFICE OF NAVAL RESEARCH
N00014-86-K-0097

EXPERIMENTAL SOLITONS

(11/01/85 – 10/31/88)

by

J. Hammack
Department of Aerospace Engineering, Mechanics & Engineering Sciences
College of Engineering
University of Florida

The goal of this research project was to study instabilities and long-time evolution of water wavetrains induced by gravitation and surface tension, i.e. gravity-capillary waves or ripples, which have frequencies in the range of 5–50 Hz on clean deep water. The research project was heavily experimental, requiring concomitant development of laboratory apparatus. Separate funding for major equipment purchases was provided by the Army ~~Research~~ Office and the Office of Naval Research through a DoD URIP grant (N00014-86-G-0201) that was entitled *Nonlinear Water Waves in Two Spatial Dimensions*. This equipment was purchased and installed during the period of this contract, and it was used in the later portion of the research program. First, ~~I summarize~~ are summarized developments of the ripple laboratory. Second, ~~I describe~~ are described some results obtained during the early period of the contract. Third, ~~I describe~~ are described some results obtained during the later period of the contract that exploited the newer laboratory apparatus. All of these results were obtained in collaboration with former students Ron Lee, Diane Henderson and Marc Perlin. Publications are attached that describe these results in more detail.

1. – The Ripple Laboratory

The ripple laboratory consists of the following: (1) wave tank, (2) wavemaker, (3) wave gauge, (4) water supply and filters, (5) two computer systems, and (6) high-speed imaging system. Items (1)–(3) and the older computer system were described in detail by Henderson & Lee (1986) and Henderson & Hammack (1987, Part 1), which are attached. The newer computer system and Item (6) were purchased and installed during the period of this contract. All of these items are described briefly below.

The wave tank was constructed of glass; it measured 91 cm wide, 183 cm long, and 15 cm deep; it was supported on the ground-floor building slab through isolation pads.

The wavemaker paddle consisted of a slender right-angled aluminum wedge that was 30.4 cm wide and supported above the water surface astride the tank's long axis; the quiescent water surface intersected its midpoint. The paddle was oscillated vertically by a mini-shaker whose motion was servo-controlled with position feedback. Parallel aluminum (wetted) sidewalls set adjacent to the paddle provided a test channel 91 cm long and 30.5 cm wide. A closed water-supply system provided deionized water that was filtered of organic materials and particulates with sizes above 0.2 μm. Water surface elevations at fixed locations in the tank were measured with *in situ* capacitance gauges.

1.1. *The computer systems.* – Our early experiments used a 16-bit DEC (Digital Equipment Corporation) MicroPDP-11 computer system for control and data acquisition. Sinusoidal command signals to the wave generator were provided by a Data Translation 12-bit analog-output system (DT2771) coupled with a DEC programmable clock (KWV11-C). Analog signals from wave gauges, command signals to the wavemaker, and position-feedback signals from the wavemaker paddle were digitized by a Data Translation 12-bit analog-input system (DT2782) coupled to a second programmable clock. Prior to digitizing, the analog signals were low-pass (Butterworth) filtered with a cutoff of 100 Hz, amplified 20 dB, high-pass filtered with a cutoff of 1 Hz, and amplified another 20 dB. Periodograms (energy spectra) of filtered analog signals were computed using fast Fourier transforms (FFT's); results were obtained in the frequency band 0–100 Hz with a resolution of 0.39 Hz.

Our later experiments used a 32-bit DEC VAXstation II for control and data acquisition. This system included a DEC 12-bit analog-output system (AAV11-DA) and a 12-bit analog-input system (ADV11-DA); each was supported by a DEC programmable clock (KWV11-C). Software support for control, data analysis, and graphical output were provided by Signal Technology's Interactive Laboratory System. Analog signals were filtered and amplified as in the earlier experiments. They were then digitized so that periodograms could be computed over the band 0–125 Hz with a resolution of 0.015 Hz.

1.2. *The high-speed imaging system.* – Quantitative spatial data were obtained in our later experiments using a Kodak EKTAPRO 1000 Motion Analyzer. This computer-based video system records images at rates up to 1000 fps (frames per second). Each frame comprises 240 × 192 pixels at which light intensity is measured with a resolution of 256 gray levels. Digitized frames were transferred from the EKTAPRO 1000 system to the VAXstation II computer system using a communications interface, which also allowed the VAXstation II to control the imaging system.

Images of wave patterns inside the test channel were obtained using an overhead camera whose focal plane was parallel to, and 1.5 m above, the water surface. The channel was lighted by two 600-W halogen lamps in reflector housings located at the downstream end of the wave tank. The lamps were positioned above the tank, astride its centerline, and aimed at the test channel so that the incident light formed an angle of

about 32° with the water surface. An opaque (white) sheet of plexi-glass was placed underneath the glass bottom of the tank in the vicinity of the test channel. The measured light intensities, which spanned 225 gray levels, were related to water depths (or wave amplitudes). Although this relationship was not known precisely, relative gray levels among pixel sites were found to yield accurate two-dimensional amplitude-wavenumber spectra when the wave amplitudes were sufficiently small and the water surface comprised a small number of wavetrains. (Comparisons between a time series of gray levels at a single pixel site and that from a nearby wave gauge yielded a linear correlation coefficient of 0.89.) Images are surrounded by a frame border that provides information on the video settings, such as the 125 fps used herein.

Although images contained 240 × 192 pixels, only 128 × 128 were used to compute the two-dimensional wavenumber (or wavevector) spectrum; these 2^{14} data points fill a (22 cm × 22 cm) area. The dimensions of the sampled area yielded a wavenumber resolution of 0.0453 cm^{-1} or 0.284 rad/cm. The physical distance between pixel sites in the images was 0.174 cm, providing a spatial sampling rate of 5.75 cm^{-1} or 36.11 rad/cm; hence, the Nyquist (spatial) frequency was 2.87 cm^{-1} or 18.06 rad/cm. This spatial frequency corresponded to a temporal frequency of 106 Hz in the experiments; temporal data showed very little energy at this frequency.

Images were obtained for analysis in the following manner. First, an experiment was performed with an *in situ* wave gauge. Then, the gauge was removed to provide an uninterrupted overhead view. The quiescent water surface was imaged, and the experiment was repeated and recorded on video tape at 125 fps. The background gray level for the quiescent water surface at each pixel site was subtracted from each image; then the mean gray level for the array was subtracted. The resulting two-dimensional array of gray levels, which provided a measure of the vertical deformation of the water surface from its quiescent position, was then used to calculate the two-dimensional wavenumber spectrum.

2. – Summary of results

First, I describe some ripple dynamics observed during the early period of this contract. These results were limited to quantitative temporal data obtained using in situ wave gauges and qualitative spatial data obtained using photography. Detailed descriptions of these results are given by Henderson & Lee (1986) and Henderson & Hammack (1987), which are attached. Second, I present a brief description of the ripple dynamics observed during the later period of this contract. These results include quantitative spatial data (two-dimensional wavenumber spectra) obtained using the imaging system. A detailed description of these results is given by Hammack Perlin, & Henderson (1988), which is also attached.

2.1 *Early Observations of Ripple Dynamics.* – Henderson & Lee (1986) investigated the generation of ripple wavetrains using a flap-type wavemaker. They solved the linear

wavemaker problem, which included some of the effects of surface tension. Their results showed that the rather extreme laboratory procedures employed in coping with surface contamination led to wave damping that compared well to predictions of the model for an "inextensible" or "fully contaminated" surface. More importantly, the experimental procedures were found to lead to reproducible results, which were essential to the research program. Henderson & Lee also encountered and documented the presence of longitudinal and transverse modulational instabilities of ripple wavetrains.

Subsequent research led to two important observations on the evolution of ripple wavetrains that were reported by Henderson & Hammack (1987). First, one-dimensional wave patterns generated at the wavemaker paddle quickly became two-dimensional, and they appeared very disordered (i.e., many length scales seemed to be present). An example of this behavior is shown in figure 1 where an overhead photograph of the water surface resulting from a 25-Hz wavetrain is shown. These two-dimensional wave patterns persisted for all ripple wavetrains with frequencies above 9.8-Hz and with sensible amplitudes. Second, when wave gauge data were obtained in the region where the wave pattern

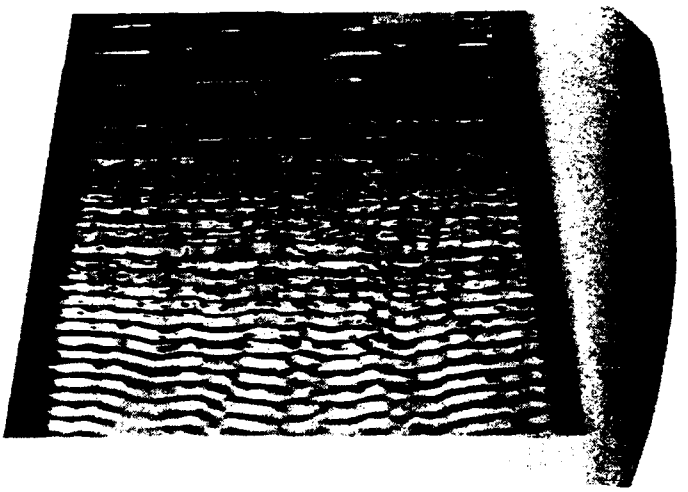

Figure 1. View of a 25-Hz wavetrain.

had become two-dimensional, and analyzed using fast Fourier transforms to find their frequency content, the results were quite simple A single resonant triad of waves appeared in the periodograms as shown in figure 2 for the 25-Hz wavetrain shown in figure 1. Three distinct waves appear in figure 2: 10-Hz, 15-Hz, and 25-Hz plus the superharmonics (50-Hz and 75-Hz) of the 25-Hz wavetrain. The selective amplification of a single (10,15,25)-Hz resonant triad was surprising since an entire continuum of triads is available to a 25-Hz wavetrain, and the theoretical model for resonant triads indicates that

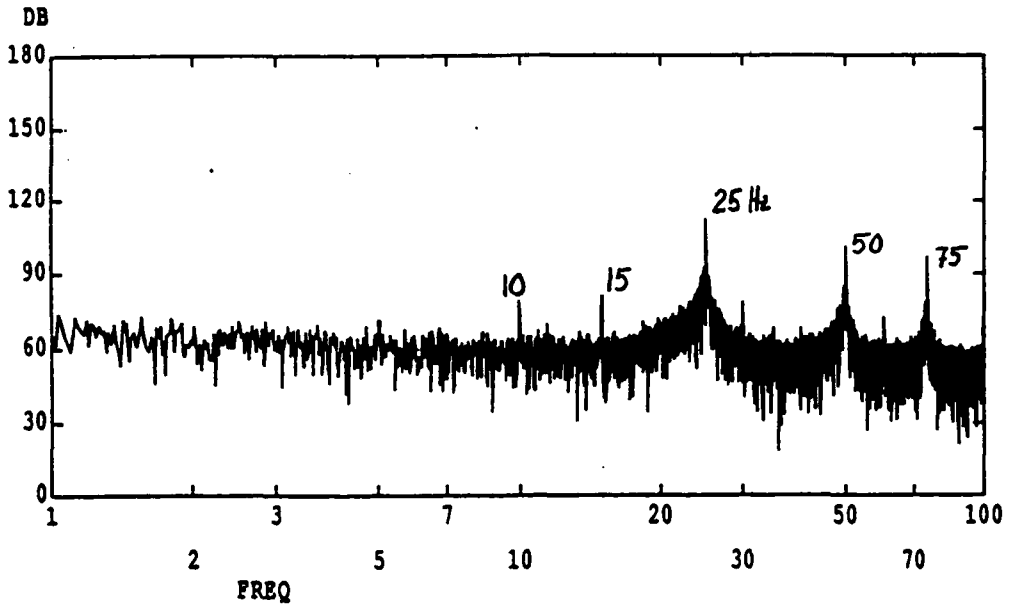

Figure 2. Periodogram of the 25-Hz wavetrain in figure 1.

all of these triads are about equally likely to be excited. (We note here that resonant triads can occur only for wavetrains with frequencies greater than 19.6 Hz on clean deep water. Below 19.6 Hz resonant quartet interactions are the first to occur, with the exception of internal resonances corresponding to Wilton ripples.)

2.2 *Later Observations of Ripple Dynamics: Temporal Data.* – When the newer computer system was installed and made operational, the earlier experiments were repeated with an unsettling result: no selective amplification was found with the newer computer in control. Analysis of the gauge measurements in the two-dimensional region of wave evolution revealed only the presence of the generated wavetrain and its superharmonics. After some effort we discovered that selective amplification was related to the presence of very small waves with high frequencies near the wavemaker. The older computer system had slightly higher levels of 60-Hz noise in its command signal to the wavemaker than that of the newer system. It was this small 60-Hz noise that seeded the wavefield in the vicinity of the wavemaker with a 60-Hz water wave. Although short-lived, the 60-Hz wave interacted with the 25-Hz wavetrain to seed the (10,15,25)-Hz triad which dominated during further evolution down the channel. (The 60-Hz water wave disappeared before reaching the first wave gauge due to viscous damping.) Even though the actual scenario by which the seed

wave selects a particular resonant triad was not completely determined during the period of this contract, it nevertheless occurred in a predictable and repeatable manner. Another example of the selection process is shown in figure 3 where an amplitude spectrum is shown for an experiment where we have artificially seeded a 25-Hz wavetrain with 57-Hz "noise" whose amplitude is $\frac{1}{10}$ that of the test wave. In this case, two triads are (predict-

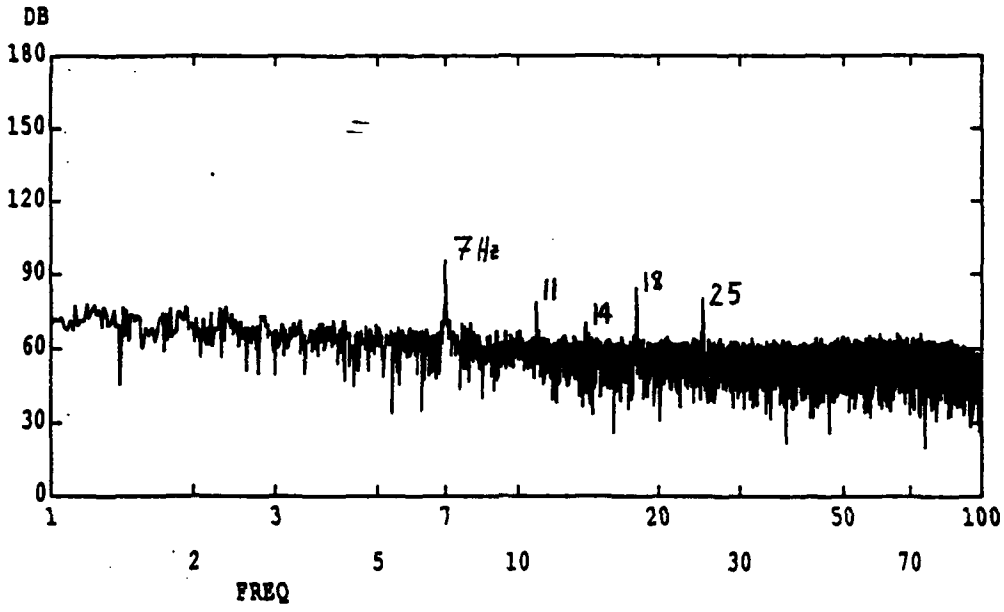

Figure 3. Periodogram for a 25-Hz wavetrain seeded by a 57-Hz wavetrain.

ably) selected: (7,18,25)-Hz and (11,14,25)-Hz. Further experiments have shown that the amplitude of the seed wave may be as little as $\frac{1}{1000}$ that of the test wave and still precipitate the triad selection process. These results have important implications for the resonant instabilities of ripples. For example, noise in the background wave field cannot be ignored when it occurs at distinct frequencies, even when its amplitude is exceedingly small. In addition, the usefulness of a well known theorem due to Hasselmann (1967, *J. Fluid Mech.* **30**, 737) is diminished when waves with amplitudes $\frac{1}{1000}$ that of the test wave are not sufficiently small to be neglected.

2.3 *Later Observations of Ripple Dynamic: Spatial Data.* – The two-dimensionality of the wave patterns visible in figure 1 is characteristic of all our ripple experiments, even when only one wavetrain (and, possibly, its superharmonics) was observed in the amplitude

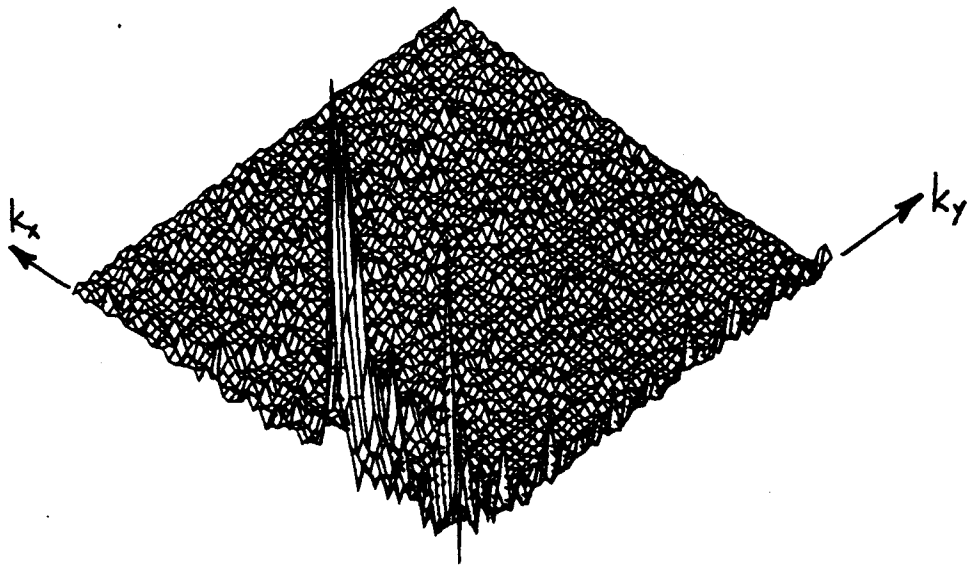

(a) perspective view

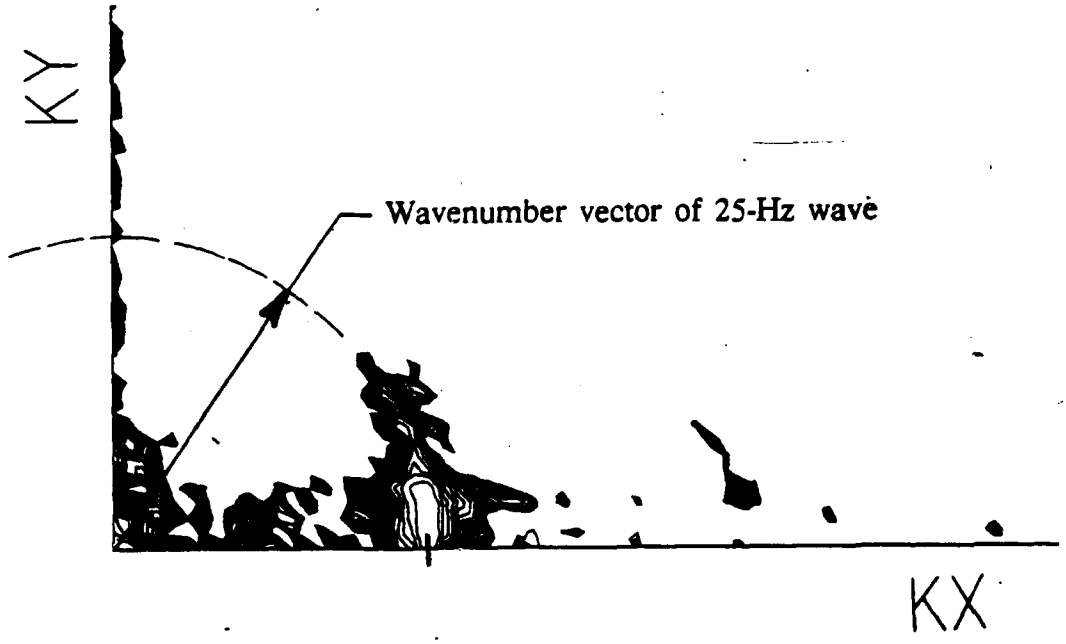

(b) contour map

Figure 4. Wavenumber spectrum for the surface pattern of a 25-Hz wavetrain.

spectrum. Understanding the origin of these two-dimensional wave patterns was provided by the *first* analysis of data from the imaging system. A spatial image of the surface pattern was obtained for a 25-Hz wavetrain generated by the newer computer system, so that only the 25-Hz wave appeared in the periodogram. The resulting spectrum of wavenumbers, k_x and k_y, in the x- and y-directions, respectively, is shown in figure 4. (The x-direction corresponds to the direction down the wave channel.) Figure 4a shows a perspective view of this spectrum while figure 4b shows a contour; the contour map is easiest to interpret. The main peak in the spectrum occurs at $k_x = 6.3\ cm^{-1}$, which corresponds to the 25-Hz wave which directed down the channel. However, note that the spectrum spreads from this point in a circular arc into the wavenumber plane. This indicates that the 25-Hz wave is spreading its energy in directions at angles to the x-axis. Hence, the two-dimensional water surface is the result of many overlapping 25-Hz waves propagating at angles to one another. We do not need waves at other frequencies to produces the irregular two-dimensional surface patterns. In fact, these patterns are not disordered, since only one length scale is present (the length of the 25-Hz waves); they only appear so to the eye. This directional instability of a ripple wavetrain appears to have gone unnoticed in previous research. Yet, it is the most dominant instability we have encountered when wave amplitudes are sensible (i.e. not exceedingly small). This result and its theoretical explanation will be studied in subsequent research.

3. - References

Henderson, D. & R. Lee 1986. Laboratory generation and propagation of ripples, **Phys. Fluids 29**(3), 619–624.

Henderson, D. & J. Hammack, 1987. Experiments on ripple instabilities. Part 1. Resonant triads, **J. Fluid Mechs. 184**, 15–41.

Hammack, J., M. Perlin, & D. Henderson, 1988. Resonant interactions among ripples. **Proceedings, International School of Physics ENRICO FERMI. Course CIX. Nonlinear Topics in Ocean Physics.** (ed. A. Osborne), to be published by North–Holland.